Proc. Natl. Acad. Sci. USA
Vol. 94, pp. 12210–12217, October 1997
Neurobiology

This contribution is part of the special series of Inaugural Articles by members of the National Academy of Sciences elected on April 25, 1995.

Defective γ-aminobutyric acid type B receptor-activated inwardly rectifying K^+ currents in cerebellar granule cells isolated from *weaver* and *Girk2* null mutant mice

PAUL A. SLESINGER*†, MARKUS STOFFEL‡, YUH NUNG JAN*, AND LILY Y. JAN*

*Howard Hughes Medical Institute, Departments of Physiology and Biochemistry, University of California, San Francisco, CA 94143-0724; and ‡Laboratory of Metabolic Diseases, The Rockefeller University, New York, NY 10021

Contributed by Lily Y. Jan, August 29, 1997

ABSTRACT **Stimulation of inhibitory neurotransmitter receptors, such as γ-aminobutyric acid type B ($GABA_B$) receptors, activates G protein-gated inwardly rectifying K^+ channels (GIRK) which, in turn, influence membrane excitability. Seizure activity has been reported in a *Girk2* null mutant mouse lacking GIRK2 channels but showing normal cerebellar development as well as in the *weaver* mouse, which has mutated GIRK2 channels and shows abnormal development. To understand how the function of GIRK2 channels differs in these two mutant mice, we compared the G protein-activated inwardly rectifying K^+ currents in cerebellar granule cells isolated from *Girk2* null mutant and *weaver* mutant mice with those from wild-type mice. Activation of $GABA_B$ receptors in wild-type granule cells induced an inwardly rectifying K^+ current, which was sensitive to pertussis toxin and inhibited by external Ba^{2+} ions. The amplitude of the $GABA_B$ receptor-activated current was severely attenuated in granule cells isolated from both *weaver* and *Girk2* null mutant mice. By contrast, the G protein-gated inwardly rectifying current and possibly the agonist-independent basal current appeared to be less selective for K^+ ions in *weaver* but not *Girk2* null mutant granule cells. Our results support the hypothesis that a nonselective current leads to the *weaver* phenotype. The loss of $GABA_B$ receptor-activated GIRK current appears coincident with the absence of GIRK2 channel protein and the reduction of GIRK1 channel protein in the *Girk2* null mutant mouse, suggesting that $GABA_B$ receptors couple to heteromultimers composed of GIRK1 and GIRK2 channel subunits.**

γ-Aminobutyric acid (GABA) is a potent inhibitory neurotransmitter that interacts with two different classes of GABA receptors: ionotropic chloride channels ($GABA_A$) and metabotropic G protein-coupled receptors ($GABA_B$) (for reviews, see refs. 1 and 2). The activation of $GABA_B$ receptors has been implicated in hippocampal long-term potentiation (3, 4), absence epilepsy (5–8), slow-wave sleep (7), muscle relaxation, and antinociception (9). $GABA_B$ receptors are expressed in both presynaptic and postsynaptic neuronal membranes, where they couple to K^+ and/or Ca^{2+} channels (2). One class of K^+ channels that are believed to couple to $GABA_B$ receptors as well as other G protein-linked neurotransmitter receptors are the G protein-gated inwardly rectifying K^+ channels (GIRK) (for reviews, see refs. 10–12).

Like all inwardly rectifying K^+ channels, GIRK channels preferentially allow more inward K^+ current to flow across the cell's membrane than outward K^+ current (13). The small outward flow of K^+ ions keeps the cell's membrane potential close to the equilibrium potential for K^+ ions (E_K), thereby affecting membrane excitability (13). Four different mammalian GIRK cDNA sequences have been identified thus far, GIRK1-GIRK4 (also referred to as Kir3.1-Kir3.4; ref. 14), and these GIRK channel subunits form heteromultimers in heterologous expression systems (15–18). Coimmunoprecipitation experiments have indicated that native G protein-gated inwardly rectifying K^+ channels in the brain are heteromultimers composed of GIRK1 and GIRK2 channel subunits (19) whereas those in the heart are heteromultimers composed of GIRK1 and GIRK4 channel subunits (17). The functional consequence of GIRK channel opening is best known in the heart, where parasympathetic activation stimulates the release of acetylcholine, which binds to muscarinic cholinergic receptors, opens atrial muscarinic GIRK channels ($I_{K(ACh)}$) and slows the heart rate (20–22). In the brain, GIRK channels also are postulated to be an important determinant of membrane excitability. Indeed, a *Girk2* null mutant mouse that lacks GIRK2 channels is more predisposed to seizures (23).

The activity of GIRK2 channels may be important in the development of the nervous system. The *weaver* mouse, in which degeneration of neurons primarily in the cerebellum and substantia nigra leads to severe ataxia, hyperactivity, and tremor (for reviews, see refs. 24 and 25), has a mutation in the *Girk2* gene (26). We reported previously that the *weaver* mutation in GIRK2 channels ($GIRK2^{wv}$) has two distinct effects on channel function in *Xenopus* oocytes: a reduction in basal and G protein-activated K^+ currents and, with high expression levels of $GIRK2^{wv}$ channels, the appearance of novel inwardly rectifying nonselective basal and G protein-activated currents (ref. 27; also see refs. 28–31). We predicted that cerebellar neurons isolated from *weaver* mice would display a reduced GIRK current and/or show an aberrant nonselective current (27). Whole-cell patch recordings from isolated *weaver* granule cells have been equivocal, however. Mjaatvedt *et al.* (32) reported that the cerebellar granule cells isolated from either wild-type or *weaver* mice do not express GIRK currents. Kofuji *et al.* (28), on the other hand, found that wild-type granule cells possess GIRK currents, but that *weaver* granule cells express an anomalous "leakage" current that is not activated by G proteins. Finally, Surmeier *et al.* (33) and Lauritzen *et al.* (34) reported that the GIRK currents in *weaver*, but not wild-type, granule cells are severely reduced. Thus, no

Abbreviations: PTX, pertussis toxin; GIRK, G protein-gated inwardly rectifying K^+ channel; GABA, γ-aminobutyric acid; GTPγS, guanosine-5′-*O*-(3-thiotriphosphate).

†To whom reprint requests should be addressed at: Box 0724, Howard Hughes Medical Institute, University of California, San Francisco, CA 94143. e-mail: sles@itsa.ucsf.edu.

consensus has been reached on the mechanism by which mutated GIRK2^{wv} channels lead to the *weaver* phenotype in the cerebellum.

To clarify the role of GIRK2 channels in cerebellar development, we examined the G protein-gated inwardly rectifying K^+ currents in cerebellar granule cells dissociated from a mutant mouse lacking GIRK2 channels (23) and compared them with the GIRK currents recorded from *weaver* granule cells. Wild-type cerebellar granule cells possess a robust GIRK current that requires pertussis toxin (PTX)-sensitive G proteins; this GIRK current is markedly reduced in both *Girk2* null mutant mice and *weaver* mutant mice. Our results support the hypothesis that the expression of an anomalous nonselective current underlies the *weaver* phenotype in cerebellar granule cells (28), rather than a loss of a K^+ current (33, 34). In addition, our results suggest that a majority of the heteromeric GIRK channels that couple to $GABA_B$ receptors in the cerebellum are composed of GIRK1 and GIRK2 channel subunits.

METHODS

Oocyte Studies. *Xenopus* oocytes were isolated as described (27). Tandem dimers of GIRK1-GIRK2 and GIRK1-GIRK2^{wv} were constructed by splicing GIRK1 at Arg-499 in-frame with GIRK2 at Leu-6 using a SSSSSSSSR linker. The GIRK2^{wv} cDNA was used as described (27). *In vitro* methyl-capped cRNA was made using T3 or T7 RNA polymerase (Stratagene), and the concentration was estimated on an ethidium-stained formaldehyde gel by comparison with a RNA molecular weight marker. Oocytes were injected with a 46-nl solution containing cRNA for m2 muscarinic receptor (≈0.2 ng) and GIRK channels (0.5–5 ng). To suppress the expression of the endogenous oocyte GIRK channel, XIR, ≈13 ng of a phosphothioated oligonucleotide (TAAATCCCTTGCCATGATGGT) antisense to XIR was coinjected with the channel cRNA in some experiments, following the protocol described by Hedin *et al.* (35). Oocytes were incubated in ND96 for 3–5 days at 18°C.

Macroscopic currents were recorded from oocytes with a two-electrode voltage-clamp amplifier (Dagan CA-1), filtered at 1 kHz, digitized (3.3 kHz) with a TL-1 A/D interface (Axon Instruments, Foster City, CA) and stored on a laboratory computer. Oocytes were perfused continuously with a solution containing 90 mM XCl (X = K^+, Na^+), 2 mM $MgCl_2$ and 10 mM Hepes (pH 7.4 with ≈5 mM XOH) with or without 500 μM $BaCl_2$. Carbachol (3 μM) (Sigma) was used to stimulate m2 muscarinic receptors. A small chamber (2 × 15 mm) with fast perfusion was used to change the extracellular solutions and was connected to ground via a 3 M KCl agarose bridge.

Granule Cell Studies. Cerebellar granule cells were isolated from cerebella of 5- to 6-day-old mouse pups. The control group consisted of C57BL/6 mice from Simonsen or littermate controls from *weaver* heterozygotes (B6CBACa-A$^{w\text{-}J}$/A-Kcnj6^{wv} from The Jackson Laboratory) matings or *Girk2* null mutant heterozygote matings (derived from F_3 and F_4 hybrid crosses of 129/sv and C57BL/6). *Weaver* mice were genotyped by using PCR cycle sequencing of the genomic DNA isolated from mouse tails to detect the *weaver* mutation (G953A). *Girk2* null mutant mice were genotyped by using PCR amplification of genomic DNA to detect the targeted sequence used for generating the *Girk2* null mutant (23). Mice were killed by decapitation using a protocol approved by the Animal Care Committee at the University of California at San Francisco. The entire cerebellar cortex was removed, sliced into small 1–2-mm pieces in Ca^{2+}- and Mg^{2+}-free PBS supplemented with 10% horse serum and 100 units/ml penicillin and 100 μg/ml streptomycin, and dissociated into single cells by trituration through fire-polished pasteur pipets. Neurons were pelleted (1,000 g) and then resuspended in MEM with Earl's basal salts supplemented with 10% horse serum (HyClone)/25 mM KCl/0.06% glucose/100 units/ml penicillin/100 μg/ml streptomycin, and plated at a density of 0.5–1 × 10^6 cells/ml on glass coverslips precoated with 25 μg/ml poly-D-lysine. Granule cells were grown at 37°C in humidified air with 5% CO_2. In some experiments, granule cells were grown in the presence of 1 μg/ml PTX (Research Biochemicals) for 18–24 hr.

The whole-cell patch clamp technique (36) was used to record macroscopic currents from granule cells grown *in vitro* for 2–3 days. Granule cells were identified based on their small size (4.0 ± 0.2 pF, n = 151), and recordings were made preferentially from neurons with short neurites to minimize problems with space-clamp. Borosilicate glass (Warner; P6165T) electrodes had resistances of 1–3 Mohms and were coated with a parafilm/mineral oil mix to reduce capacitance. Membrane currents were recorded with an Axopatch 200A amplifier (Axon Instruments), adjusted electronically for cell capacitance and series resistance (80–100%), filtered at 2 kHz with a Bessel filter, digitized at 5 kHz with a TL-1 interface (Axon Instruments), and stored on a laboratory computer. Intracellular pipet solution contained 120 mM KCl, 20 mM NaCl, 5 mM EGTA, 10 mM glucose, 2.56 mM K_2ATP, 5.46 mM $MgCl_2$ and 10 mM Hepes (pH 7.2 with ≈14 mM KOH). With these ion concentrations, ≈140 mM K^+, 2 mM free Mg^{2+} and 2 mM MgATP were in the intracellular solution. Either 300 μM Li_3-GTP (Boehringer) or 100–150 μM Li_3-guanosine-5′-*O*-(3-thiotriphosphate) (GTPγS) (Research Biochemicals) was added to the intracellular pipet solution. The external bath solution (20K) contained 140 mM NaCl, 20 mM KCl, 5 mM glucose, 0.5 mM $CaCl_2$, 2 mM $MgCl_2$, and 10 mM Hepes (pH 7.2). In some experiments, external Na^+ was replaced with *N*-methyl-D-glucamine. The osmolarity was 310–330 mOsm. The bath solution sometimes contained 0.2–200 μM (±)-baclofen (Research Biochemicals), or 500 μM $BaCl_2$ (Aldrich). The bath solution was perfused locally using gravity flow through a 1.14-mm polyethylene tube connected to a Teflon manifold (Warner). Current voltage relations and reversal potential measurements were corrected for the junction potential of ≈5 mV, estimated using the Junction Potential Calculator (Axon Instruments). The zero-current potential (reversal potential) was measured only in granule cells that displayed G protein-activated inwardly rectifying currents evoked by either incremental voltage steps or a continuous change in voltage (ramps).

All reported values are mean ± SEM. Statistical analyses were performed with unpaired Student's t test or with ANOVA followed by an appropriate posthoc test (SigmaStat 2.0).

RESULTS

Expression of GIRK Channels in Oocytes. We found previously that *Xenopus* oocytes injected with cRNA for GIRK2^{wv} channels produced channels that lose their selectivity for K^+ ions, giving rise to basal and G protein-activated Na^+ currents (27). Coexpression of GIRK1 channel subunits with GIRK2^{wv} channel subunits gave rise to markedly reduced basal and muscarinic receptor-activated K^+ currents as compared with oocytes expressing GIRK1 and wild-type GIRK2 channels subunits, suggesting that heteromultimers composed of GIRK1 and GIRK2^{wv} channel subunits were functionally impaired (27). To test this possibility, we constructed tandem dimers in which the GIRK1 channel subunit was linked in frame with either the GIRK2 or GIRK2^{wv} channel subunit. Oocytes injected with the GIRK1-GIRK2 dimer cRNA and the m2 muscarinic receptor cRNA expressed an inwardly rectifying basal K^+ current that was reversibly inhibited by 500 μM external $BaCl_2$, eliminated by replacing all of the external K^+ with Na^+ ions, and enhanced by muscarinic receptor stimulation (Fig. 1 *A*, *C*, and *D*). Expression of the GIRK2^{wv} cRNA with the muscarinic receptor cRNA in oocytes gave rise to a large inward basal current that was reduced by external Ba^{2+} ions and enhanced by muscarinic stimulation, but decreased only slightly when K^+ ions were replaced with Na^+ ions (Fig. 1 *B* and *C*; cf ref. 27). The GIRK2^{wv} channels apparently retain the pore property of susceptibility to inhibition by external

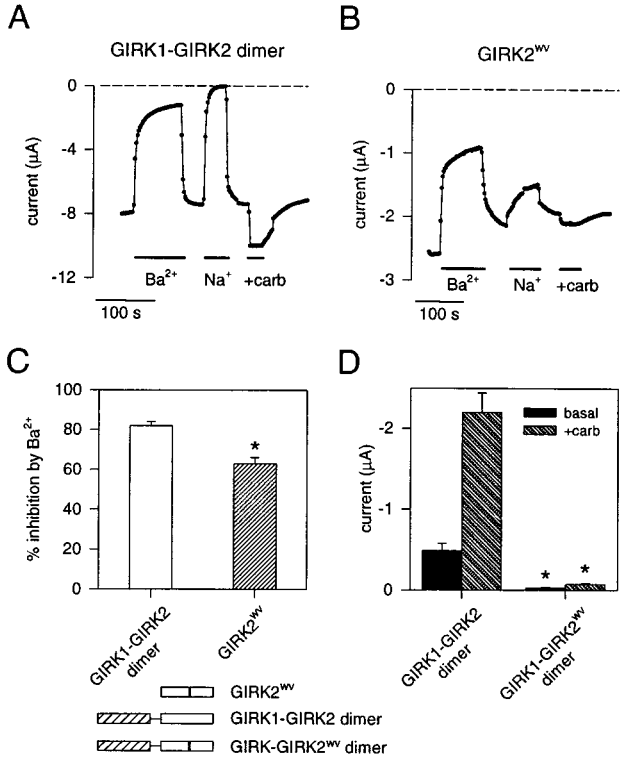

FIG. 1. GIRK2^{wv} channel subunits are nonselective whereas GIRK1-GIRK2^{wv} dimers fail to produce detectable GIRK currents when expressed in *Xenopus* oocytes. Inward currents were measured with two-electrode voltage-clamp from oocytes injected with cRNA for the m2 muscarinic receptor along with the cRNA for either the GIRK1-GIRK2 wild-type dimer, GIRK1-GIRK2^{wv} dimer, or the GIRK2^{wv} channel subunit. The current at −100 mV is plotted as a function of time for oocytes expressing the GIRK1-GIRK2 wild-type dimer (*A*) and the GIRK2^{wv} channel (*B*). Oocytes were perfused continuously with a solution containing 95 mM K^+. Solid bar indicates exposure to 95 mM K^+ + 500 μM $BaCl_2$ ($+Ba^{2+}$), 95 mM Na^+ ($+Na^+$), or 95 mM K^+ + 3 μM carbachol (+carb). (*C*) The percentage of the basal current that was inhibited by 500 μM $BaCl_2$ for GIRK1-GIRK2 dimer (82% ± 2%, $n = 3$) and for GIRK2^{wv} channel (63% ± 3%, $n = 4$). * indicates $P < 0.05$ as determined by Student's unpaired *t* test. (*D*) The average current measured at −100 mV in the absence (basal) and then presence of carbachol (+carb) in oocytes expressing GIRK1-GIRK2 dimer (-0.49 ± 0.09 μA for basal; −2.20 ± 0.24 μA for +carbachol; $n = 7$) or GIRK1-GIRK2^{wv} dimer (-0.03 ± 0.01 μA for basal; −0.07 ± 0.01 μA for +carbachol; $n = 9$). Current was adjusted for linear leakage current. * indicates that the basal and +carbachol currents for GIRK1-GIRK2^{wv} dimer are statistically smaller than those for GIRK1-GIRK2 dimer ($P < 0.05$ as determined by ANOVA followed by Dunn's posthoc test on ranks).

Ba^{2+} ions even though the channels have lost their selectivity for K^+ ions. The GIRK1-GIRK2^{wv} dimer, by contrast, showed a small basal current and no enhancement with muscarinic receptor stimulation (Fig. 1*D*). To suppress the expression of the endogenous GIRK channel, XIR (35), which potentially could coassemble with the GIRK1-GIRK2 dimers, we also coinjected an oligonucleotide (KHA1) that was antisense to XIR with the dimer cRNA. The oligonucleotide KHA1 was shown to reduce the formation of GIRK multimers that contain the endogenous subunit XIR (35). Expression of the GIRK1-GIRK2^{wv} dimer with KHA1 again failed to produce inwardly rectifying currents that could be enhanced by muscarinic receptor stimulation (−0.22 ± 0.02 μA in the presence of carbachol for GIRK1-GIRK2^{wv} dimer vs. −1.57 ± 0.32 μA for GIRK1-GIRK2 dimer, $n = 5$). These results suggest that heteromultimers composed of two GIRK1 channel subunits and two GIRK2^{wv} channel subunits (i.e., two dimers) are functionally silent, due to either impaired channel function, formation, or membrane targeting.

G Protein-Gated Inwardly Rectifying K^+ Currents in Wild-Type Cerebellar Granule Cells. Wild-type granule cells possess a large rapidly inactivating voltage-gated K^+ current (cf. ref. 37) that was largely suppressed by shifting the membrane holding potential from −80 mV to 0 mV (Fig. 2 *A* and *B*). The depolarized holding potential revealed an inwardly rectifying current that was inhibited completely by 500 μM $BaCl_2$ (Fig. 2 *A* and *B*) and reversed near the equilibrium potential for K^+, indicating the presence of an inwardly rectifying K^+ current (Fig. 2 *A* and *B*). The inward K^+ current increased with time and reached a steady-state level (Fig. 2*C*) with GTPγS in the intracellular solution, as expected from the persistent G protein activation by the nonhydrolyzable GTP analogue. The GTPγS-activated current was completely and reversibly blocked by 500 μM $BaCl_2$ (Fig. 2 *C* and *D*). Both the GTPγS-activated and Ba^{2+}-sensitive currents showed strong inward rectification (Fig. 2*D*). Thus, cerebellar granule cells express a G protein-gated inwardly rectifying K^+ current.

We next examined whether GIRK currents could be activated through stimulation of G protein-coupled neurotransmitter receptors. We chose baclofen, a $GABA_B$ receptor agonist, because $GABA_B$ receptors are expressed in the developing cerebellum (38) and because activation of $GABA_B$ receptors had been shown to inhibit Ca^{2+} channels in cultures of cerebellar neurons (39, 40). Unlike the recordings with GTPγS, the basal inward current did not increase with time when GTP was included in the intracellular recording solution (Fig. 3*A*). Application of the $GABA_B$ agonist (±)-baclofen reversibly enhanced the inward current in a dose-dependent fashion (Fig. 3*A*). Like the GTPγS-activated inwardly rectifying K^+ current, the current induced by (±)-baclofen showed strong inward rectification and reversed near the K^+ equilibrium potential of −50 mV (Fig. 3*B*). The dose-response curve for the (±)-baclofen-activated GIRK currents had a K_D of 16 μM and a Hill coefficient of ≈1 (Fig. 3*C*).

Because $GABA_B$ receptors are coupled to both PTX-sensitive and PTX-insensitive G proteins (2), we examined the PTX sensitivity of the $GABA_B$ receptor-activated currents in cerebellar granule cells. Pretreatment of granule cells with 1 μg/ml PTX suppressed the baclofen-activated GIRK currents (Fig. 3 *D* and *E*). Thus, GIRK channels are present in the cerebellum and are coupled to neurotransmitter receptors via PTX-sensitive G proteins, similar to the GIRK channels in heart (41).

GTPγS-Activated GIRK Currents in *weaver* and *Girk2* Null Mutant Cerebellar Granule Cells. Similar to their fate *in vivo*, granule cells dissociated from homozygous *weaver* mouse cerebellum (*wv/wv*) failed to extend long neurites and died *in vitro* within 4 days of the isolation, consistent with the findings reported by Willinger *et al.* (42). The GTPγS-activated currents therefore were recorded from granule cells grown *in vitro* for only 2–3 days. Whereas the inward current in *wv/wv* granule cells changed little with time, the inward current in the *+/wv* neuron increased during the recording, similar to +/+ granule cells. This change in inward current was not due to a change in the leakage current because the outward current through the voltage-gated K^+ channels did not show a corresponding increase (not shown) and the GTPγS-activated current displayed strong rectification, similar to that of the GTPγS-activated current in wild-type granule cells (Fig. 4 *B* and *D*). The amplitude of the GTPγS-activated current in both *+/wv* and *wv/wv* granule cells was significantly smaller than that of the wild-type granule cells (Fig. 4*E*).

Although the reduction in the amplitude of GTPγS-activated current was evident in both *weaver* and *Girk2* null mutant granule cells, the reversal potential for the GIRK current was shifted to membrane potentials more depolarized than E_K for *+/wv* (Fig. 4*D*, *Inset*) and *wv/wv* granule cells. The mean reversal potential for the GTPγS-activated current in *+/wv* and *wv/wv* granule cells was −31 ± 6 mV ($n = 7$) and −32 ± 6 mV ($n = 3$), respectively, as compared with −52 ± 3 mV ($n = 11$) for +/+ granule cells.

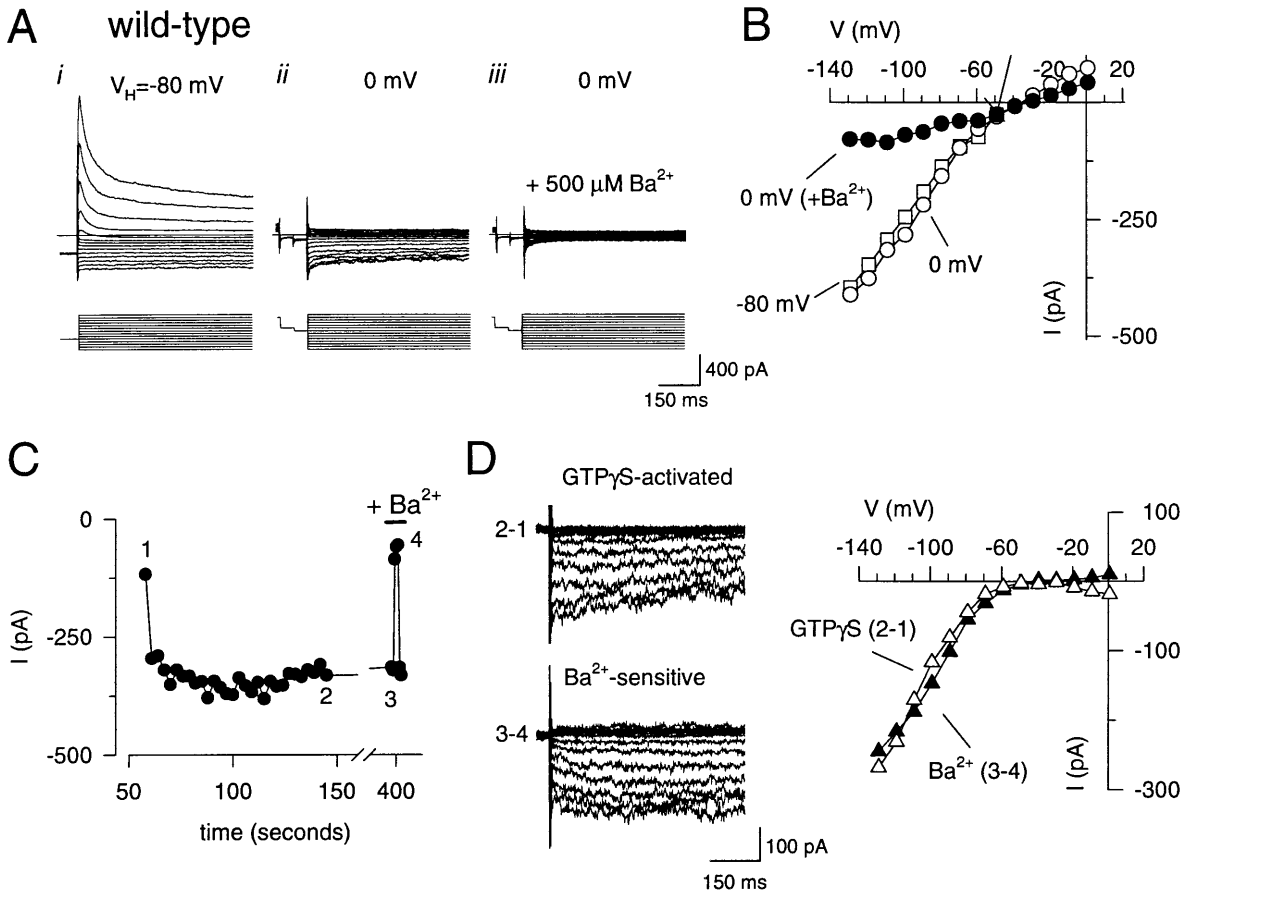

FIG. 2. Cerebellar granule cells possess GTPγS-activated inwardly rectifying K^+ currents that are inhibited by external Ba^{2+}. Whole-cell currents were recorded from a wild-type cerebellar granule cell with 20 mM K^+ in the extracellular solution and 140 mM K^+ in the intracellular solution (E_K= −50 mV). (*A*) Whole-cell currents were elicited by voltage steps from −120 to +10 mV in 10 mV increments from a holding potential of −80 mV (*i*) or 0 mV (*ii* and *iii*). In some cases, a prepulse to −40 mV(50 ms) and then −50 mV (50 ms) was delivered before the test pulse to monitor the leakage current. A depolarized holding potential suppresses the rapidly inactivating voltage-gated K^+ current and reveals an inwardly rectifying K^+ current. Inclusion of 500 μM $BaCl_2$ in the extracellular solution inhibits the inwardly rectifying K^+ current (*iii*). (*B*) The current is plotted as a function of the membrane potential for 0 mV (○), −80 mV (□), and 0 mV in the presence of Ba^{2+} (●). (*C*) The inward current at −120 mV is plotted as a function of time after the beginning of the whole-cell recording. Numbers near points indicate the time points used for deriving the difference currents in *D*. (*D*) The GTPγS-activated (△) current was obtained by subtracting the current recorded at the beginning of the whole-cell recording (1) from the current recorded after GTPγS activation (2). The Ba^{2+}-sensitive (▲) current was obtained by subtracting the current recorded during exposure to 500 μM $BaCl_2$ (3) from the control current before $BaCl_2$ (4). The current-voltage plots show that both GTPγS-activated (△) and Ba^{2+}-sensitive (▲) currents displayed strong rectification and reversed near the equilibrium potential for K^+ (E_K), indicating strong K^+ selectivity. The extracellular solution contained 20 mM K^+ and 145 mM *N*-methyl-D-glucamine. All current recordings were compensated electronically for cell capacitance and series resistance.

Such a shift in the reversal potential is expected for channels that lose their selectivity for K^+ ions. Thus, the GTPγS-activated currents in +/*wv* and *wv*/*wv* granule cells are not strongly selective for K^+ ions. Consistent with our studies on the heterologous expression of GIRK1 and GIRK2^{wv} channel subunits in *Xenopus* oocytes (27), the *weaver* mutation appears to have a dual effect on GIRK currents in cerebellar granule cells: a reduction in the amplitude of the GTPγS-activated GIRK currents and a change in K^+ selectivity.

In contrast to *wv*/*wv* granule cells, granule cells isolated from *Girk2* −/− cerebellum survived *in vitro* and extended long neurites, similar to wild-type neurons. Inclusion of GTPγS in the pipet led to little or no activation of GIRK currents in *Girk2* −/− granule cells (Fig. 4 *C* and *E*). The amplitude of the GTPγS-activated currents recorded from *Girk2* +/− granule cells was not significantly different from that of wild-type granule cells (Fig. 4*E*), indicating that one copy of the *Girk2* gene was sufficient to produce GTPγS-activated GIRK currents. In contrast to the GTPγS-activated currents in +/*wv* granule cells, the GTPγS-activated current in *Girk2* +/− granule cells reversed at −51 ± 2 mV (n = 11), indicating normal K^+ selectivity.

$GABA_B$ Receptor-Activated GIRK Currents in *weaver* and *Girk2* Null Mutant Cerebellar Granule Cells. We next compared the Ba^{2+}-sensitive basal (agonist-independent) currents and the $GABA_B$ receptor-activated currents in *Girk2* null mutant granule cells with those in *weaver* granule cells. To reduce the possibility that the neurons that possessed a large GIRK2^{wv} current would die rapidly *in vitro*, we examined the GIRK currents in *weaver* granule cells grown with QX-314 to delay the onset of cell death (28). The amplitude of the agonist-independent basal inward K^+ current in the +/*wv* and *wv*/*wv* granule cells was not significantly different from that in +/+ granule cells (Fig. 5). By contrast, the amplitude of the baclofen-activated current was significantly reduced in *wv*/*wv* granule cells and completely absent in −/− granule cells, as compared with +/*wv*, +/−, and +/+ granule cells (Fig. 5*D*). Examples of recordings in which stimulation of $GABA_B$ receptors with (±)-baclofen in *wv*/*wv* and −/− granule cells resulted in no response are shown (Fig. 5 *B* and *C*). As was found for the GTPγS activated GIRK currents, the amplitude of the baclofen-induced currents was markedly reduced in *wv*/*wv* and −/− granule cells, as compared with wild-type granule cells (Fig. 5*D*). Surprisingly, the reversal potential for the baclofen-activated current in +/*wv* granule cells was not significantly

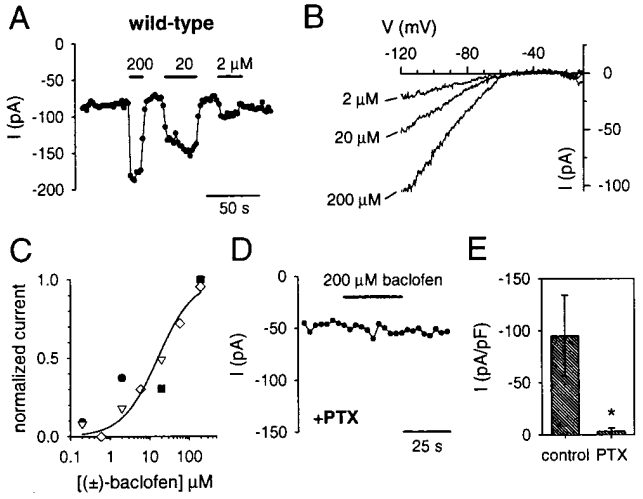

FIG. 3. $GABA_B$ receptor-activated inwardly rectifying K^+ currents require PTX-sensitive G proteins in wild-type granule cells. (*A*) The inward current measured at −120 mV from a holding potential of 0 mV is plotted as a function of time. Solid bar indicates exposure to 200, 20, or 2 μM (±)-baclofen. Note the increase in inward current during activation of $GABA_B$ receptors. (*B*) The baclofen-activated currents were obtained by subtracting the basal (agonist-independent) current from the current measured in the presence of baclofen. The current was elicited by a voltage ramp pulse from −120 mV to +20 mV (0.64 V/s) from a holding potential of 0 mV. The extracellular solution contained 20 mM K^+ and 145 mM Na^+. All of the baclofen-activated currents reversed (zero-current potential) near −50 mV, the equilibrium potential for K^+, and showed strong rectification (little outward current positive to −50 mV). (*C*) (±)-baclofen dose-response curve. The change in inward current at −120 mV produced by different concentrations of baclofen was normalized to the change in current produced by 200 μM baclofen and plotted as a function of baclofen concentration. Each symbol represents a different recording. Smooth curve shows the best fit using the Hill equation ($I = 1/(1+(K_D/[\text{baclofen}])^a)$, with a K_D of 16 μM and a Hill coefficient (a) of 0.95. (*D*) The inward current measured at −120 mV in a granule cell pretreated for 16–20 hr with 1 μg/ml PTX is plotted as a function of time. No induction of current was seen with 200 μM baclofen (solid bar). (*E*) The average baclofen-activated currents were normalized to the cell capacitance for control granule cells (−95 ± 39 pA/pF; $n = 5$) and granule cells pretreated with PTX (−3.2 ± 3.3 pA/pF; $n = 6$). * indicates statistical significance ($P < 0.05$) using unpaired Student's *t* test.

different from that of wild-type granule cells (−56 ± 2 mV for +/+ vs −51 ± 3 mV for +/*wv*), even though the GTPγS-activated GIRK currents in +/*wv* granule cells were significantly less selective (see *Discussion*).

In some recordings, both *wv*/*wv* and −/− granule cells displayed a large basal current even though there was little or no detectable $GABA_B$ receptor-activated inwardly rectifying K^+ current. This agonist-independent current was reversibly inhibited by 500 μM $BaCl_2$ (Fig. 5 *A–C*) and reversed near the equilibrium potential for K^+ ions in +/+, +/*wv*, and −/− granule cells (Fig. 5*E*), indicating strong selectivity for K^+ ions. Interestingly, the reversal potential for the Ba^{2+}-sensitive inwardly rectifying current in *wv*/*wv* granule cells showed much larger variability than that for +/+ or +/− granule cells, but the mean was not significantly different from +/+ or −/− granule cells (Fig. 5*E*).

DISCUSSION

Cerebellar granule cells possess a robust G protein-activated inwardly rectifying K^+ current that is coupled to $GABA_B$ receptors through PTX-sensitive G proteins. Because the GIRK currents are eliminated or reduced in both *wv*/*wv* and −/− granule cells and because *wv*/*wv*, but not −/−, mice show severe cerebellar atrophy, it is unlikely that the loss of GIRK current causes the *weaver* phenotype. Rather, the presence of a G protein-activated inwardly rectifying nonselective current and possibly an agonist-independent nonselective basal current may underlie the expression of the *weaver* phenotype. Our finding that the loss of $GABA_B$ receptor-activated currents occurs in mice that lack GIRK2 channel and most GIRK1 channel subunits suggests that GIRK1-GIRK2 heteromultimers form a majority of GIRK channels that couple to postsynaptic $GABA_B$ receptors in cerebellar granule cells. These GIRK1-GIRK2 heteromultimers may underlie the $GABA_B$ receptor-activated slow inhibitory postsynaptic potential in the mouse brain.

GIRK Currents in Wild-Type Cerebellar Granule Cells. Cerebellar granule cells isolated from 5-day-old mice exhibited both GTPγS-activated and $GABA_B$ receptor-activated inwardly rectifying K^+ currents, corroborating previous reports of GIRK currents in these neurons (28, 33, 34). At present, we cannot explain why Mjaatvedt *et al.* (32) failed to record G protein-gated inwardly rectifying K^+ currents. The $GABA_B$ receptor-mediated activation of GIRK current requires PTX-sensitive G proteins. Similar findings have been reported for CA3 hippocampal neurons (43). Thus, $GABA_B$ receptors probably use $G_{\alpha i}/G_{\alpha o}$ G proteins for GIRK activation in the brain. Several features of the GIRK currents in cerebellar granule cells differ from the GIRK currents in hippocampal neurons, however. The GIRK currents in cerebellar granule cells show strong rectification, reminiscent of the strong rectification observed in oocytes expressing the GIRK1-GIRK2 dimer. By contrast, the GIRK currents in hippocampal CA3 neurons did not rectify strongly (43). This difference could be due to the washout of polyamines, which are known to affect inward rectification (44). Alternatively, the subunit composition of GIRK channels in the hippocampus may differ from that in the cerebellum. Both GIRK1 and GIRK2 channel subunits are expressed in the developing cerebellum and hippocampus (19, 27). However, the developmental expression pattern for other GIRK subfamily members is not known and potentially could affect the rectification properties of the heteromultimers.

Another difference between the hippocampal and cerebellar GIRK currents is the kinetics of the time-dependent change in inward current during sustained hyperpolarizations. In hippocampal CA3 neurons, the currents activated rapidly (43), similar to the time-dependent change in current observed in oocytes expressing GIRK2 channel subunits (16, 27). In some cerebellar granule cells, the GTPγS-activated inward K^+ currents activated slowly upon hyperpolarization to negative membrane potentials (Fig. 4). Slow activation also was observed for the $I_{K(ACh)}$ current in cardiac myocytes (45) and for the currents in oocytes coexpressing GIRK1-GIRK2 or GIRK1-GIRK4 heteromultimers (16, 27, 46). Because high levels of GIRK1 and GIRK2 mRNA and only low levels of GIRK4 mRNA are expressed in the cerebellum (47), the slowly activating GIRK current in granule cells may arise from channels composed predominantly of GIRK1 and GIRK2 subunits. However, the GIRK current activated quickly upon hyperpolarization in other granule cells (Fig. 2), suggesting that some GIRK currents may be carried by GIRK2 homomultimers or possibly channels with other combinations of GIRK channel subunits.

Defective GIRK Currents in Both *weaver* and *Girk2* Null Mutant Cerebellar Granule Cells. One of the major defects in both the heterozygote and homozygote *weaver* granule cells is a dramatic reduction in the amplitude of the GTPγS-activated as well as the baclofen-activated GIRK current. A reduction in the amplitude of the G protein-activated GIRK current in *wv*/*wv* granule cells also has been observed in other studies (28, 33, 34). To learn more about the possible mechanism underlying the loss of a GIRK current, we examined the expression of a GIRK1-GIRK2^{wv} dimer in *Xenopus* oocytes. In contrast to the GIRK1-GIRK2 wild-type dimer, the expression of GIRK1-GIRK2^{wv}

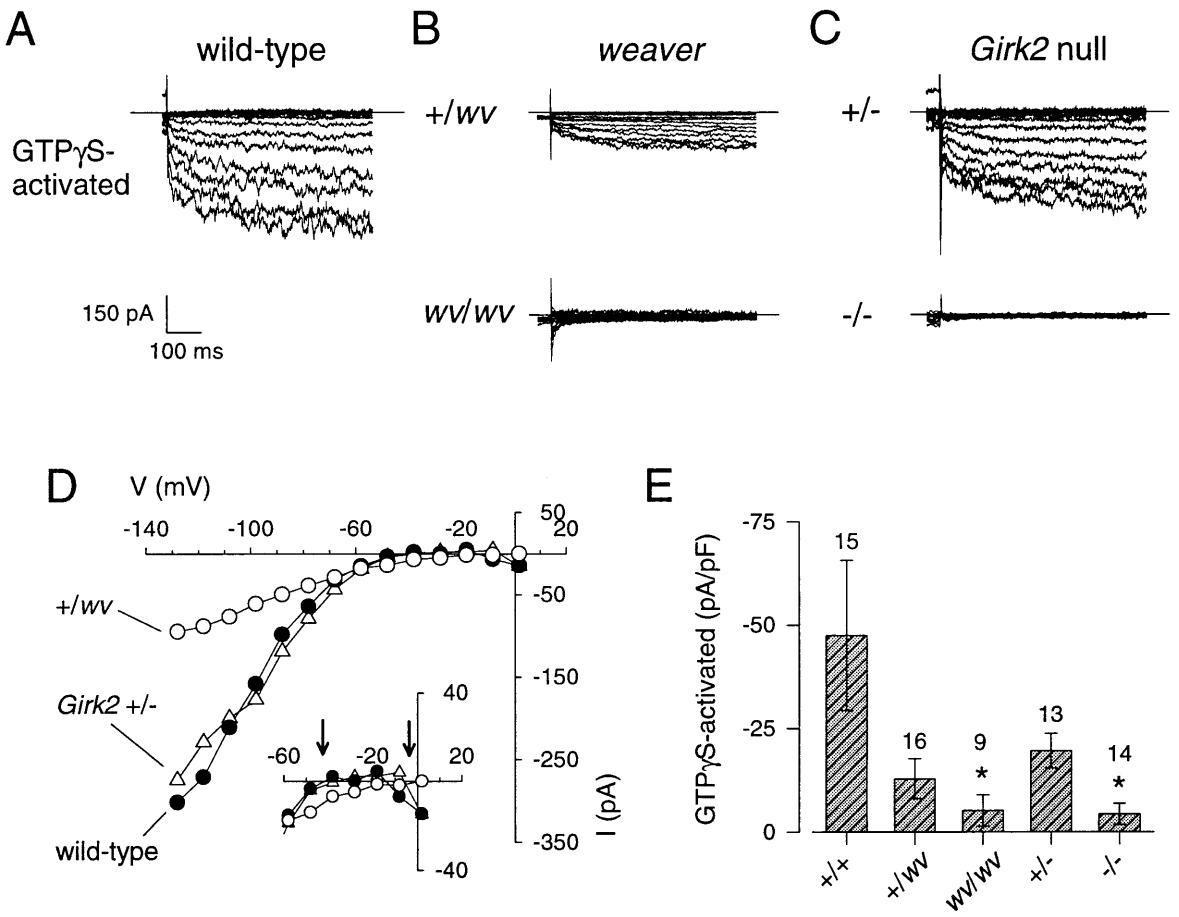

FIG. 4. GTPγS-activated currents are markedly reduced in granule cells isolated from *weaver* and *Girk2* null mutant mice, but only *weaver* granule cells show a change in K^+ selectivity. Examples of GTPγS-activated currents recorded from wild-type (*A*), *weaver* (*B*), and Girk2 null (*C*) mutant mice are shown. Currents were elicited by voltage steps from −130 to +10 mV from a holding potential of 0 mV. The extracellular solution contained 20 mM K^+ and 145 mM Na^+. The GTPγS-activated current was obtained by subtracting the current recorded at the beginning of the whole-cell recording from the current recorded after GTPγS activation (see Fig. 2 legend). (*D*) The current-voltage plots show the strong rectification for +/+, +/−, and +/*wv* granule cells but a reversal potential for the +/*wv* granule cell that was more depolarized than that for the +/+ or +/− granule cells (arrows, *Inset*). (*E*) Bar graph shows the mean (±SEM) amplitude of the GTPγS-activated currents divided by the cell capacitance for +/+, +/*wv*, *wv*/*wv*, +/−, and −/− granule cells. Number of recordings is indicated above bars. * indicates significant difference from +/+ ($P < 0.05$) as determined by one-way ANOVA followed by Dunn's posthoc test on ranks.

dimer failed to produce basal or G protein-activated GIRK currents. If GIRK channels form tetramers, like their G protein-insensitive counterparts (48), then the results suggest that GIRK channels composed of two GIRK1 subunits and two $GIRK2^{wv}$ subunits are functionally silent, due to impaired channel function, formation, or membrane targeting. The large reduction in the amplitude of GIRK currents in the *weaver* granule cells therefore can be explained by the functional impairment of heteromultimers, such as a GIRK1-$GIRK2^{wv}$–GIRK1-$GIRK2^{wv}$ tetramer. The functional impairment of heteromultimers containing $GIRK2^{wv}$ channels could be one mechanism for mitigating the toxic effects of mutant channels. A change in the sensitivity of heteromultimers containing $GIRK2^{wv}$ channels to activation by the G protein $G_{\beta\gamma}$ subunits also may contribute to the smaller G protein-activated inwardly rectifying K^+ currents (29).

In addition to the dramatic reduction in the amplitude of the GIRK current, we observed a variable change in the ionic selectivity for the GIRK currents in *weaver* granule cells. In a small number of granule cells that expressed a detectable GTPγS-activated GIRK current, the GTPγS-activated GIRK current reversed at membrane potentials more depolarized than E_K, indicating that the GIRK channels lost some selectivity for K^+ ions. Surprisingly, a similar shift in the reversal potential occurred in both +/*wv* and *w*/*wv* granule cells even though the failure to differentiate and the subsequent cell death is more severe in the *wv*/*wv* granule cells as compared with the +/*wv* granule cells (25). However, the granule cells that are more severely affected by the $GIRK2^{wv}$ channels in the *wv*/*wv* cultures likely were missed in our study because we restricted our analysis to recordings from only viable granule cells. Unexpectedly, whereas the GTPγS-activated GIRK currents in +/*wv* granule cells clearly showed a change in selectivity, the reversal potential for the $GABA_B$ receptor-activated currents in +/*wv* granule cells was not significantly different from that of wild-type granule cells. One possible explanation for this finding is that the $GIRK2^{wv}$ containing channels that have reduced K^+ selectivity are not activated by $GABA_B$ receptors, but are accessible to other G proteins (GTPγS will activate all of the G proteins in a cell). For example, $GIRK2^{wv}$ homomultimers or other GIRK heteromultimers may not couple efficiently to $GABA_B$ receptors but would be activated by GTPγS.

In addition to the G protein-activated inwardly rectifying K^+ current, some granule cells also possess a basal inwardly rectifying K^+ current that is sensitive to inhibition by external Ba^{2+}. Although the GTPγS-activated component of current in *weaver* was less selective for K^+, we could not detect a consistent change in the reversal potential for the Ba^{2+}-sensitive basal current in *wv*/*wv* granule cells. It is possible that the GIRK currents in *weaver* granule cells were not sensitive

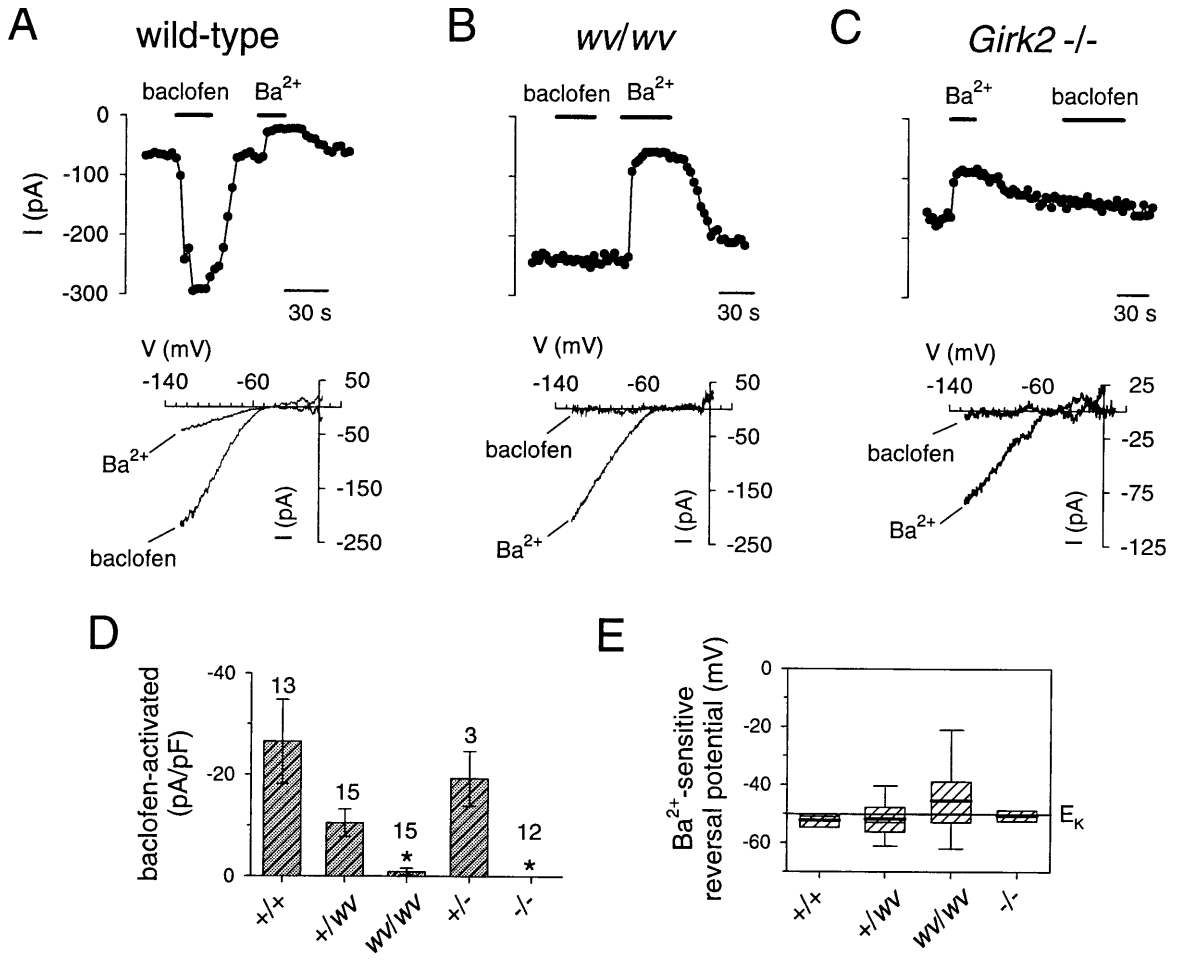

FIG. 5. *Girk2* −/− mutant and *wv/wv* mutant granule cells lack $GABA_B$ receptor-activated K^+ currents but not Ba^{2+}-sensitive inwardly rectifying basal K^+ currents. The inward current at −120 mV elicited by voltage ramps from −120 mV to +50 mV is plotted as a function of time for +/+ (*A*), *wv/wv* (*B*), and −/− (*C*) granule cells. Solid bar indicates exposure to the extracellular solution (20 mM K^+ and 145 mM Na^+) containing 200 μM (±)-baclofen or 500 μM $BaCl_2$. The holding potential was 0 mV. Note that the inward current changed little during exposure to baclofen in −/− and *wv/wv* granule cells, whereas the basal current was inhibited by 500 μM $BaCl_2$. The current-voltage relations (*Lower*) show that the Ba^{2+}-sensitive current rectifies strongly and reverses near −50 mV, indicating strong K^+ selectivity. (*D*) Bar graph plots the mean amplitude of the baclofen-activated inwardly rectifying K^+ currents (at −120 mV) after normalization to the cell capacitance for the various mutants. * indicates significant difference ($P < 0.05$) from +/+ using one-way ANOVA followed by Dunn's post hoc test on ranks. Number of recordings is indicated above bars. (*E*) Box plot shows the mean (solid bar), median (thin bar), 25th and 75th percentiles (box), and 10th and 90th percentiles (capped error bars) for the reversal potential of the Ba^{2+}-sensitive inward current. The mean reversal potential for the Ba^{2+}-sensitive current was −52 ± 3 mV ($n = 3$) for +/+, −52 ± 3 mV ($n = 9$) for +/*wv*, −46 ± 5 mV ($n = 8$) for *wv/wv*, and −51 ± 2 mV ($n = 3$) for −/− granule cells. The mean amplitude of the agonist-independent basal current was −18.6 ± 3.8 pA/pF for +/+, −35.1 ± 6.6 pA/pF for +/*wv*, −33.1 ± 7.5 pA/pF for *wv/wv*, −13.0 ± 3.2 pA/pF for +/−, and −14.8 ± 3.6 pA/pF for −/− granule cells. Granule cells isolated from *wv/wv* mice were cultured with 100 μM QX-314 to delay the onset of cell death.

to inhibition by external Ba^{2+}; however, this explanation is unlikely because oocytes expressing $GIRK2^{wv}$ channels gave rise to nonselective inwardly rectifying currents that were inhibited by Ba^{2+}. Alternatively, the Ba^{2+}-sensitive basal current could arise from both G protein-sensitive nonselective channels and G protein-insensitive inwardly rectifying K^+ channels, making it difficult to measure the shift in selectivity. In addition to GIRK1, GIRK2, and GIRK3 channels, the G protein-insensitive inwardly rectifying K^+ channel IRK2 is expressed in the mouse brain (47, 49). Thus, if both K^+ selective and nonselective channels are present in *wv/wv* granule cells, we would expect the currents to reverse at membrane potentials more depolarized than E_K but vary between −50 and 0 mV depending on the proportion of K^+ selective to nonselective channels. Indeed, Surmeier *et al.* (33) found that the ratio of the Ba^{2+}-sensitive Na^+ current to the Ba^{2+}-sensitive K^+ current was more variable in *wv/wv* granule cells than in +/+ granule cells.

Since the identification of a mutated GIRK2 channel in the *weaver* mouse (26), considerable debate has been waged over the mechanism by which mutant $GIRK2^{wv}$ channels lead to the *weaver* phenotype; hypotheses have ranged from a loss of a GIRK current (33, 34) to the expression of a novel nonselective current (28) to other factors unrelated to GIRK2 expression (32, 50, 51). In our experiments, the amplitude of the G protein-activated inwardly rectifying K^+ current was severely attenuated in granule cells isolated from both *Girk2* −/− mutant and from *wv/wv* mutant mice. Yet, the cerebellum in *Girk2* −/− mutant mice develops normally (23) and the survival of isolated granule cells grown *in vitro* is not impaired, in contrast to *weaver* mice. Thus, our results favor the hypothesis that the change in K^+ selectivity of the GTPγS-activated GIRK current and possibly the agonist-independent basal current is the cellular event that culminates in the *weaver* phenotype in cerebellar granule cells. It remains to be determined whether the toxicity arises from excessive Na^+ influx and/or Ca^{2+} influx due to mutant $GIRK2^{wv}$ channels.

GIRK1-GIRK2 Heteromultimers May Underlie $GABA_B$ Receptor-Mediated Slow Inhibitory Postsynaptic Potential. *Girk2* −/− mutant cerebellar granule cells failed to show any

$GABA_B$ receptor-activated inwardly rectifying K^+ currents, but occasionally displayed a GTPγS-activated GIRK current. The small GTPγS-activated current that remains in $-/-$ granule cells could arise from the formation of heteromultimers that lack GIRK2 subunits, such as heteromultimers composed of GIRK1 and GIRK3 channel subunits, but do not couple efficiently to $GABA_B$ receptors. The association of GIRK1 and GIRK2 channel subunits does occur *in vivo* because antibodies directed against GIRK1 channel subunits coimmunoprecipitate GIRK2 channel subunits in the cerebral cortex, hippocampus, and cerebellum (19). In the *Girk2* null mutant mouse that lacks GIRK2 channel protein, a marked reduction in GIRK1 channel protein (23) as well as a loss of $GABA_B$ receptor-activated currents in both the hippocampus (52) and the cerebellum (this study) is found. Taken together, these observations suggest that GIRK1-GIRK2 heteromultimers form one of the major effectors for $GABA_B$ receptors.

What is the physiological significance of GIRK channel activity in the brain? One clue comes from studies on hippocampus where $GABA_B$ receptors have been implicated in a slow inhibitory postsynaptic potential (53). Lüscher *et al.* (52) have found that hippocampal neurons no longer exhibit a slow $GABA_B$-mediated inhibitory postsynaptic potential in *Girk2* null mutant mice. Thus, GIRK1-GIRK2 channels may be primarily responsible for the postsynaptic inhibition mediated by $GABA_B$ receptors in the mouse brain.

We thank H. A. Lester for providing m2 receptor cDNA, M. Lazdunski for providing mGIRK2 cDNA in a high expression vector, R. Nicoll and C. Lüscher for reading the manuscript, and E. Wolff for her technical assistance. This work was supported by a National Institute of Mental Health Silvio Conte Neuroscience Center grant at the University of California at San Francisco (Y.N.J. and L.Y.J.). Y.N.J. and L.Y.J. are Howard Hughes Investigators.

1. Bowery, N. G. (1993) *Annu. Rev. Pharmacol. Toxicol.* **33,** 109–147.
2. Misgeld, U., Bijak, M. & Jarolimek, W. (1995) *Prog. Neurobiol.* **46,** 423–462.
3. Davies, C. H., Starkey, S. J., Pozza, M. F. & Collingridge, G. L. (1991) *Nature (London)* **349,** 609–611.
4. Mott, D. D. & Lewis, D. V. (1991) *Science* **252,** 1718–1720.
5. Hosford, D. A., Clark, S., Cao, Z., Wilson, W. A., Jr., Lin, F. H., Morrisett, R. A. & Huin, A. (1992) *Science* **257,** 398–401.
6. Liu, Z., Vergnes, M., Depaulis, A. & Marescaux, C. (1992) *Neuroscience* **48,** 87–93.
7. McCormick, D. A. & Bal, T. (1994) *Curr. Opin. Neurobiol.* **4,** 550–556.
8. Snead, O. C. (1992) *Eur. J. Pharmacol.* **213,** 343–349.
9. Malcangio, M. & Bowery, N. G. (1995) *Clin. Neuropharmacol.* **18,** 285–305.
10. Hille, B. (1992) *Neuron* **9,** 187–195.
11. Nicoll, R. A., Malenka, R. C. & Kauer, J. A. (1990) *Physiol. Rev.* **70,** 513–565.
12. North, R. A. (1989) *Br. J. Pharmacol.* **98,** 13–28.
13. Hille, B. (1992) *Ionic Channels of Excitable Membranes* (Sinauer, Sunderland, MA).
14. Doupnik, C. A., Davidson, N. & Lester, H. A. (1995) *Curr. Opin. Neurobiol.* **5,** 268–277.
15. Duprat, F., Lesage, F., Guillemare, E., Fink, M., Hugnot, J.-P., Bigay, J., Lazdunski, M., Romey, G. & Barhanin, J. (1995) *Biochem. Biophys. Res. Commun.* 657–663.
16. Kofuji, P., Davidson, N. & Lester, H. A. (1995) *Proc. Natl. Acad. Sci. USA* **92,** 6542–6546.
17. Krapivinsky, G., Gordon, E. A., Wickman, K., Velimirovic, B., Krapivinsky, L. & Clapham, D. E. (1995) *Nature (London)* **374,** 125–141.
18. Velimirovic, B. M., Gordon, E. A., Lim, N. F., Navarro, B. & Clapham, D. E. (1996) *FEBS Lett.* **379,** 31–37.
19. Liao, Y. J., Jan, Y. N. & Jan, L. Y. (1996) *J. Neurosci.* **16,** 7137–7150.
20. Harris, E. J. & Hutter, O. F. (1956) *J. Physiol.* **133,** 58P–59P.
21. Loewi, O. (1921) *Pflügers Arch.* **189,** 239–242.
22. Trautwein, W. & Dudel, J. (1958) *Pflügers Arch.* **266,** 324–334.
23. Signorini, S., Liao, Y. J., Duncan, S. A., Jan, L. Y. & Stoffel, M. (1997) *Proc. Natl. Acad. Sci. USA* **94,** 923–927.
24. Herrup, K. (1996) *Proc. Natl. Acad. Sci. USA* **93,** 10541–10542.
25. Hess, E. J. (1996) *Neuron* **16,** 1073–1076.
26. Patil, N., Cox, D. R., Bhat, D., Faham, M., Myers, R. M. & Peterson, A. S. (1995) *Nat. Genet.* **11,** 126–129.
27. Slesinger, P. A., Patil, N., Liao, Y. J., Jan, Y. N., Jan, L. Y. & Cox, D. R. (1996) *Neuron* **16,** 321–331.
28. Kofuji, P., Hofer, M., Millen, K. J., Millonig, J. H., Davidson, N., Lester, H. A. & Hatten, M. E. (1996) *Neuron* **16,** 941–952.
29. Navarro, B., Kennedy, M. E., Velimirovic, B., Bhat, D., Peterson, A. S. & Clapham, D. E. (1996) *Science* **272,** 1950–1953.
30. Tong, Y., Wei, J., Zhang, S., Strong, J. A., Dlouhy, S. R., Hodes, M. E., Ghetti, B. & Yu, L. (1996) *FEBS Lett.* **390,** 63–68.
31. Tucker, S. J., Pessia, M., Moorhouse, A. J., Gribble, F., Ashcroft, F. M., Maylie, J. & Adelman, J. P. (1996) *FEBS Lett.* **390,** 253–257.
32. Mjaatvedt, A. E., Cabin, D. E., Cole, S. E., Long, L. J., Breitwieser, G. E. & Reeves, R. H. (1995) *Genomic Res.* **5,** 453–463.
33. Surmeier, D. J., Mermelstein, P. G. & Goldowitz, D. (1996) *Proc. Natl. Acad. Sci. USA* **93,** 11191–11195.
34. Lauritzen, I., DeWeille, J., Adelbrecht, C., Lesage, F., Murer, G., RaismanVozari, R. & Lazdunski, M. (1997) *Brain Res.* **753,** 8–17.
35. Hedin, K. E., Lim, N. F. & Clapham, D. E. (1996) *Neuron* **16,** 423–429.
36. Hamill, O. P., Marty, A., Neher, E., Sakmann, B. & Sigworth, F. J. (1981) *Pflügers Arch.* **391,** 85–100.
37. Zegarra-Moran, O. & Moran, O. (1994) *Exp. Brain Res.* **98,** 298–304.
38. Turgeon, S. M. & Albin, R. L. (1993) *Neuroscience* **55,** 311–323.
39. Amico, C., Marchetti, C., Nobile, M. & Usai, C. (1995) *J. Neurosci.* **15,** 2839–2848.
40. Huston, E., Scott, R. H. & Dolphin, A. C. (1990) *Neuroscience* **38,** 721–729.
41. Pfaffinger, P. J., Martin, J. M., Hunter, D. D., Nathanson, N. M. & Hille, B. (1985) *Nature (London)* **317,** 536–538.
42. Willinger, M., Margolis, D. M. & Sidman, R. L. (1981) *J. Supramol. Struct. Cell. Biochem.* **17,** 79–86.
43. Sodickson, D. L. & Bean, B. P. (1996) *J. Neurosci.* **16,** 6374–6385.
44. Lopatin, A. N., Makhina, E. N. & Nichols, C. G. (1994) *Nature (London)* **372,** 366–369.
45. Simmons, M. A. & Hartzell, H. C. (1987) *Pflügers Arch.* **409,** 454–461.
46. Reuveny, E., Slesinger, P. A., Inglese, J., Morales, J. M., Iniguez-Lluhi, J. A., Lefkowitz, R. J., Bourne, H. R., Jan, Y. N. & Jan, L. Y. (1994) *Nature (London)* **370,** 143–146.
47. Karschin, C., Dissmann, E., Stuhmer, W. & Karschin, A. (1996) *J. Neurosci.* **16,** 3559–3570.
48. Yang, J., Jan, Y. N. & Jan, L. Y. (1995) *Neuron* **15,** 1441–1447.
49. Horio, Y., Morishige, K., Takahashi, N. & Kurachi, Y. (1996) *FEBS Lett.* **379,** 239–243.
50. Gao, W. Q., Liu, X. L. & Hatten, M. E. (1992) *Cell* **68,** 841–854.
51. Liesi, P. & Wright, J. M. (1996) *J. Cell. Biol.* **134,** 477–486.
52. Lüscher, C., Jan, L. Y., Stoffel, M., Malenka, R. C. & Nicoll, R. A. (1997) *Neuron*, in press.
53. Dutar, P. & Nicoll, R. A. (1988) *Nature (London)* **332,** 156–158.